UDK 542.057:544.526.5:549.514.6:620.3:549.282
Original scientific article/Izvirni znanstveni članek

ISSN 1580-2949
MTAEC9, 52(4)443(2018)

SYNTHESIS AND EFFICIENT PHOTOCATALYTIC ACTIVITY OF Ag-NANOPARTICLES-DECORATED MESOPOROUS TiO_2 SPHERES

SINTEZA IN UČINKOVITA FOTOKATALITIČNA AKTIVNOST MEZOPOROZNIH TiO_2 KROGLIC, DEKORIRANIH Z Ag NANODELCI

Shu Cui[1,2], Yanjuan Li[1], Haixin Zhao[1], Nan Li[1], Xiaotian Li,[1] Guodong Li[1,3]

[1]Jilin University, College of Material Science and Engineering, Key Laboratory of Automobile Materials of Ministry of Education, 2699 Qianjin Street, Changchun, 130012, China
[2]Tonghua Normal University, School of Physics, Tonghua, 134002, China
[3]Jilin University, College of Chemistry, State Key Laboratory of Inorganic Synthesis and Preparative Chemistry, Changchun 130012, China
xiaotianli@jlu.edu.cn

Prejem rokopisa – received: 2017-12-04; sprejem za objavo – accepted for publication: 2018-01-25

doi:10.17222/mit.2017.206

Nano-heterostructures that integrate the advantages of nanomaterials and heterojunctions have attracted wide interest in photocatalysis. Herein, heterostructured Ag-nanoparticles-decorated mesoporous TiO_2 spheres (Ag/m-TiO_2) photocatalyst has been successfully prepared by a facile method. The results show that numerous Ag nanoparticles with diameters less than 5 nm dispersed homogenously onto the mesoporous TiO_2 spheres and consequently form heterostructures. N_2 adsorption-desorption measurements indicate that the resultant products were porous with highly specific surface area. When used to photodegradate methylene blue (MB), the Ag/m-TiO_2 heteroarchitecture exhibits significantly enhanced photocatalytic performance compared with mesoporous TiO_2 spheres (m-TiO_2). Furthermore, the photocatalytic mechanism also has been discussed.

Keywords: titanium oxide, heterostructure, photocatalytic performance

Nanoheterostrukture, ki združujejo dobre lastnosti nanomaterialov in heterospojev, so pritegnile pozornost raziskovalcev fotokatalize. V prispevku avtorji opisujejo enostavno metodo za uspešno pripravo fotokatalizatorja, in sicer z Ag nanodelci dekoriranih mezoporoznih TiO_2 kroglic (Ag/m-TiO_2). Rezultati karakterizacije so pokazali, da so se številni Ag nanodelci s premerom manj kot 5 nm homogeno razpršili na mezoporozne TiO_2 kroglice. Posledično so tako nastale heterostrukture. Adsorpcijsko-desorpcijske N_2 meritve nakazujejo, da so bili nastali produkti porozni z zelo specifično površino. Heterostruktura Ag/m-TiO_2 kaže občutno povečano fotokatalitično učinkovitost v primerjavi z mezoporoznimi TiO_2 kroglicami (m-TiO_2) pri njegovi porabi za fotodegradacijo metilenskega modrila (MB). Nadalje avtorji v članku razpravljajo še o fotokatalitičnih mehanizmih.

Ključne besede: titanov oksid, heterostruktura, fotokatalitična učinkovitost

1 INTRODUCTION

TiO_2 has been applied in the fields of biocompatibility, sunscreen, inorganic pigment, solar cells, sensors and catalysis due to its high physical and chemical stability, non-toxicity, and strong availability, as well as effectiveness.[1–5] So far, TiO_2 photocatalytic technology has demonstrated that it is a valid treatment of refractory organic wastewater.[6–10] However, the anatase TiO_2 band gap is 3.2 eV, its absorption threshold is 387.5 nm, in the ultraviolet region.[11] Expanding the adsorption range to the visible region 400–800 nm is an urgent target. The nano-heterostructure has drawn intense considerations in environmental pollution controlling area, because it can overcome the two obstacles of TiO_2 photocatalyst: the dissatisfactory quantum efficiency and the negligable utilization of visible light. In the last few years, a number of materials have been combined with TiO_2 to form heterostructure to improve the photo-conversion efficiency of TiO_2, such as Ag,[12] Au,[13] CdS,[14] WO_3.[15]

The literature has demonstrated that loading of noble metal nanoparticles is an effective stratagy for enhancing the photocatalytic performance. Relative to other noble metals, Ag is attracting enormous research interest due to its low-cost and non-toxicity. As well known, Ag particles can act as electron acceptor centers and separate electron and hole pairs.[16] Simultaneously, its Fermi level is lower than that of the conduction band of TiO_2, which can drastically improve the photocatalytic property of TiO_2 and increase the quantum yield for photocatalytic processes.[17] As we all know, the size of Ag particles has a great effect on the photocatalytic properties. Reducing the particles' diameter to nano-size is an effective proposal to improve their specific surface area, and consequently the benefits for their performances in lots of surface-related applications. Studies have already confirmed that,[8,9,18,19] loading silver on the solid carrier to form a composite catalyst is a powerful approach to prevent particles from agglomeration, and enhance the photocatalytic activity.

In previous work we have successful synthesized mesoporous TiO_2 spheres and Ag_3PO_4/TiO_2 heteroarchitecture,[20] and the composite catalysts exhibit excellent photocatalytic performance under visible light. Herein, we demonstrate the synthesis of nano-heterostructured Ag/mesoporous TiO_2 spheres (Ag/m-TiO_2) photocatalyst via a facile and effective method. Profiting from the unique structure with large pores and the relative high specific surface area of the mesoporous TiO_2 spheres, the resultant products were investigated as photocatalysts in the degradation of methylene blue under both the UV light and UV-visible light.

2 EXPERIMENTAL PART

2.1 Synthesis of mesoporous TiO_2 spheres

The mesoporous TiO_2 spheres (m-TiO_2) were obtained by combining the sol-gel method with the solvothermal method, as our previous report.[20]

2.2 Fabrication of Ag/m-TiO_2 heterostructured photocatalyst

First, 70 mg m-TiO_2 spheres were added into 50 mL 2×10^{-3} M silver-ammonia ($[Ag(NH_3)_2]NO_3$) aqueous solution with ultrasonics for 30 min and then the mixture was kept under a mechanical stir for a while at room temperature to make the $[Ag(NH_3)_2]^+$ ions fully absorbed on the m-TiO_2 surfaces via the electrostatic attraction. After that, 15 mL PVP ethanol solution was added and refluxed at 70 °C for 3 h. The final products were centrifuged, washed with ethanol and deionized water, and then dried at 60 °C. The products denoted as Ag-1/m-TiO_2.

In addition, the same procedures were performed for the synthesis of sample Ag-2/m-TiO_2 and Ag-3/m-TiO_2, in which the concentrations of $[Ag(NH_3)_2]NO_3$ are 2×10^{-2} M and 2×10^{-1} M, respectively.

2.3 Structural characterizations

X-ray diffractions (XRD) were operated on a D8 Tools X-ray diffractometer using Cu-$K\alpha$ radiation (λ = 0.154056 nm). The morphology and microstructure of the as-prepared samples were observed by scanning electron microscope (SEM/EDS, JEOL JSM-6700F) and transmission electron microscope (TEM, JEM 3010 and Tecnai G2 F20). The porosity of the samples was analyzed at 77 K by nitrogen adsorption-desorption using the Barrett–Joyner–Halenda (BJH) method on a Quantochrome Autosorb 1 sorption analyzer. The Brunauer–Emmett–Teller (BET) measurement was used to evaluate the specific surface area. X-Ray photoelectron spectroscopy (XPS) was performed by a VG ESCALAB LKII instrument with Mg KR-ADES (hν = 1253.6 eV) source at a residual gas pressure of below 10^{-8} Pa. A PerkinElmer spectrometer using KBr pellets was adopted to record the Fourier transform infrared (FTIR) spectra. UV–Vis diffuse reflectance spectroscopy (DRUV-VIS) of the resultant products was characterized by a spectrophotometer Bws003 in the range 190–800 nm and used $BaSO_4$ as a reference standard.

2.4 Photocatalytic property testing of Ag/m-TiO_2

A 120 mL of MB solution with different concentrations of 30 mg L^{-1} (ultraviolet light) and 10 mg L^{-1} (visible light) in the presence of a certain amount of solid catalyst (12 mg for ultraviolet light and 60 mg visible light) was put into the photoreactor with light source and coolant system, in which the internal light source was a 50 W high-pressure mercury lamp and a 300 W halogen lamp. In order to make an adsorption-desorption equilibrium, the solution was kept stirring in dark conditions for half an hour. In the test process, aliquots of dispersion with given intervals of illumination were taken out for investigation. UV/Vis spectroscopy (UV-2550PC) was used to monitor the degradation of the MB. In the calculation of the photocatalytic activities, C and C_0 stand for the real time concentration of MB and the initial concentration respectively.

3 RESULTS

3.1 Structural features and morphology

XRD was used to determine the crystallographic structures of the m-TiO_2 and Ag-1/m-TiO_2. All diffraction of m-TiO_2 sphere (**Figure 1a**) peaks at 2θ = 38.2°, 44.3°, 64.4°, and 77.4° can be readily indexed to anatase TiO_2, which is consistent with the data JCPDS 21-1272. From the calculation from the Scherrer equation, the crystallite size of TiO_2 particles is 8.2±1.6 nm. After loading with Ag, no peaks of Ag are observed (**Figure 1b**), indicating the Ag is in the nanosize.

Typical SEM images of the m-TiO_2 spheres and Ag-1/m-TiO_2 hybrid spheres are represented in **Figure 2**.

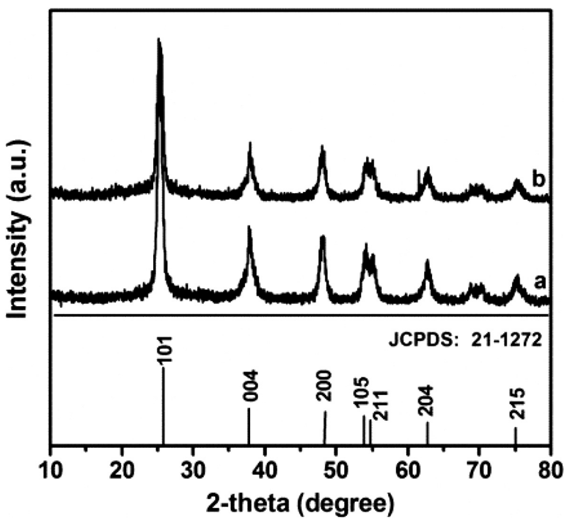

Figure 1: XRD patterns of m-TiO_2: a) and Ag-1/m-TiO_2, b) composites; peaks of JCPDS 21-1272 are shown for comparison

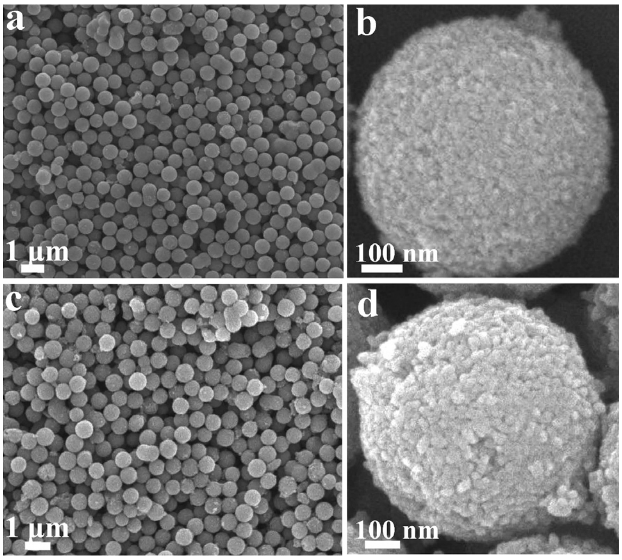

Figure 2: SEM images of: a, b) m-TiO_2 and c, d) Ag-1/m-TiO_2

The m-TiO_2 spheres composed of numerous nanoparticles have good dispersion with uniform diameter of ϕ750 nm (**Figures 2a** and **2b**). After loading of Ag nanoparticles (Ag NPs), the diameters and morphologies show no obvious changes (**Figures 2c** and **2d**), indicating the Ag particles are very small and well dispersed.

In order to observe clearly, the Ag-1/m-TiO_2 was characterized by TEM as shown in **Figure 3**. Observed from the low magnification of the TEM (**Figure 3a**), no Ag particles can be found on the surface of the sphere, attributed to the small size and the good distribution of the Ag particles. Further observations from HRTEM image (**Figure 3b**) illustrate that there are numerous nanoparticles less than 10 nm attached on the edge of each TiO_2 particle. This result reveals the formation of Ag-TiO_2 heterostructure, where metallic nano-size Ag and TiO_2 layer join. In addition, two sets of lattice fringes of 0.345 nm and 0.238 nm are assigned to the TiO_2 and Ag respectively (JCPDS card.[21] 21-1272 and JCPDS card. 04-0783).[21] To further confirm the presence and distribution of Ag NPs on the TiO_2 microspheres, electron mapping analysis was shown in **Figures 3c** to **3f**. A variety of color distributions displayed as parts of **Figures 3d** to **3f**, confirm the Ti-, O-, and Ag-enriched areas of the sample, respectively, suggesting Ag has been successfully loaded on the surface of TiO_2 and dispersed homogenously. The EDS analysis (**Figure 3g**) of the Ag-1/m-TiO_2 microspheres illustrates the existence of Ti, O and Ag elements and the percent of Ag is 5 %.

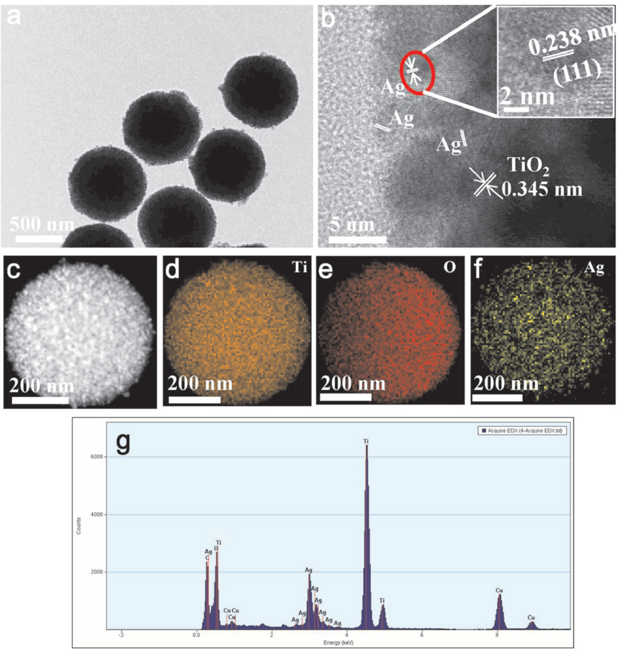

Figure 3: TEM images of Ag-1/m-TiO_2: a) low resolution and b) high resolution, c) TEM mapping images of the Ag-1/m-TiO_2 microspheres, d) Ti, e) O, and f) Ag element mapping images of the Ag-1/m-TiO_2 microspheres, g) the corresponding EDS image

Figure 4 shows nitrogen adsorption properties of m-TiO_2 and Ag-1/m- TiO_2. The m-TiO_2 has a type-IV curve with a H1 hysteresis loop, corresponding to the mesoporous characteristic.[22] The feature of the curve shows not much change after Ag loading, indicating the mesoporous structure is maintained after incorporating the Ag. However, the BET specific surface areas and pore volumes all reduce with the inclusion of Ag NPs. Before loading of the Ag, the specific surface areas and

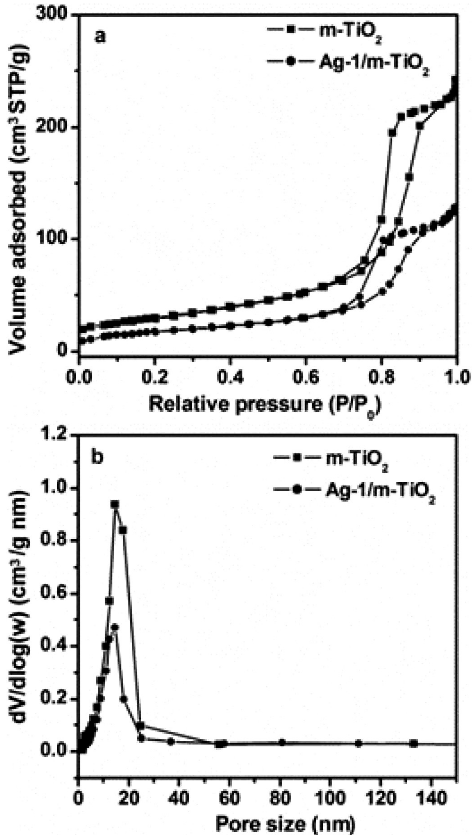

Figure 4: a) Nitrogen adsorption–desorption isotherm and b) the corresponding pore size distribution of m-TiO_2 and Ag-1/m- TiO_2

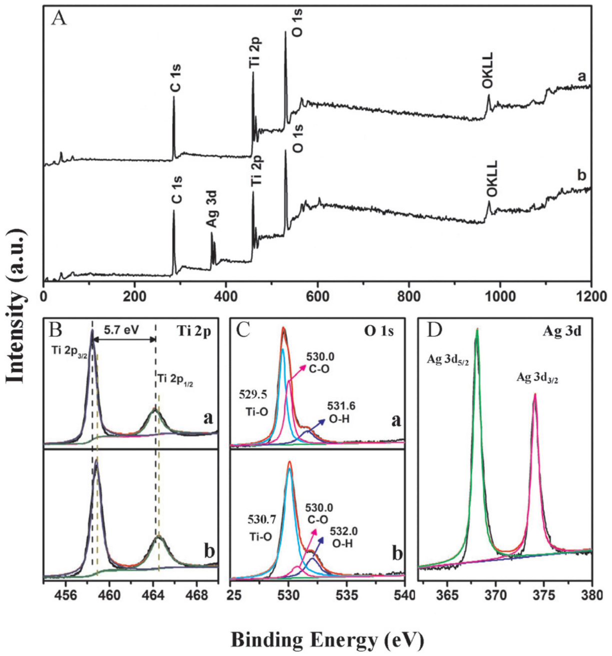

Figure 5: XPS spectra: a) fully scanned spectra, b) Ti 2p, c) O 1s, d) Ag 3d

pore volume values of m-TiO_2 are 107.9 m^2/g and 0.366 cm^3/g. But Ag-1/m-TiO_2 has a specific surface area and pore volume of 64.4 m^2/g and 0.200 cm^3/g. In the pore size distribution curves, samples m-TiO_2 microsphere and Ag-1/m-TiO_2 present a similar narrow distribution, which are in the range of 0–22 nm (**Figure 4b**). The average pore sizes of both samples are 12 nm. A previous report demonstrated that loading metal in the mesostructures would result in the remarkable perturbation in the surface area,[23] pore volume, and pore size respects. But the same phenomenon was not observed in this case, suggesting the good dispersion and small size of Ag NPs in the m-TiO_2.

XPS has been recognized as a useful measurement for qualitatively determining the surface component and composition for the samples. **Figure 5a** exhibits the fully scanned spectra from 0 eV to 1200 eV, illustrating that the Ag-1/m-TiO_2 sample is comprised of C, Ti, O and Ag. Since the C element is usually ascribed to an adventitious carbon-based contaminant. To harvest further evidences for the a) m-TiO_2 and b) Ag-1/m-TiO_2 interaction between the Ag nanocrystals and m-TiO_2 support, the high-resolution XPS spectra of Ti 2p, O1s and Ag 3d are shown in the **Figures 5b** to **5d**. **Figure 5b** is the high-resolution spectrum of Ti 2p, two typical peaks lie in 458.8 eV and 464.5 eV are pointed to the oxidation state of Ti^{4+} in anatase TiO_2. As **Figure 5c** shows, the O 1s curve can be fitted into three peaks located at (530.0, 530.7 and 532.1) eV, which corresponds to the lattice oxygen from the C–O, the OH species resulting from H_2O and Ti–O bond in bulk TiO_2,[24] respectively. More specially, the peak positions for Ti 2p and O 1s of the Ag-1/m-TiO_2 hybrids shift to higher binding energy

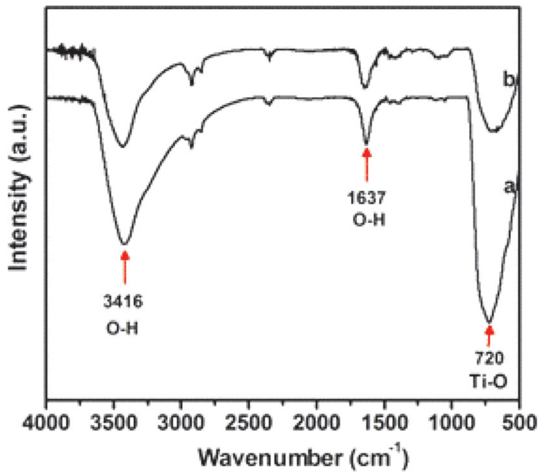

Figure 6: FT-IR spectra of: a) m-TiO_2 and b) Ag-1/m-TiO_2

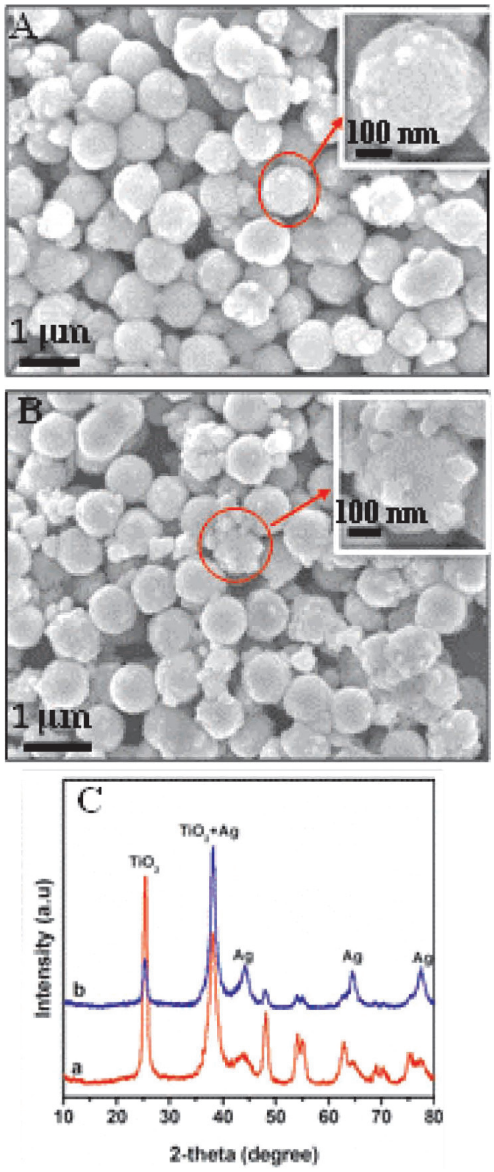

Figure 7: SEM images of: a) Ag-2/m-TiO_2, b) Ag-3/m-TiO_2, c) XRD spectra of Ag-2/m-TiO_2, and Ag-3/m-TiO_2

bands than those in pure m-TiO_2, which is due to the presence of the oxygen vacancy, resulting in a lower electron density for the Ti and O atoms in Ag-1/m-TiO_2 hybrids, and it is beneficial for improving the photocatalytic performance. In order to confirm the chemical status of Ag, the corresponding high-resolution XPS spectrum is shown in **Figure 5d**. There are two individual peaks centered at 368.1 eV and 374.1 eV could be attributed to Ag 3d5/2 and Ag 3d3/2, and the splitting of 3d doublet is 6.0 eV. This result proves that Ag is certainly present in the form of metallic Ag in the hybrids.[25]

The FT-IR spectra of m-TiO_2 and Ag-1/m-TiO_2 are displayed in **Figure 6**. In general, the spectrum of the Ag-1/m-TiO_2 resembles that of m-TiO_2. The absorption bands located at 3416 cm^{-1} and 1632 cm^{-1} in both spectra are assigned to O-H group in H_2O. The IR absorptions appear at 720 cm^{-1} are caused by the Ti-O stretching mode.[26] Although the spectra of m-TiO_2 and Ag-1/m-TiO_2 are similar, the intensity of the Ti-O in Ag-1/m-TiO_2 significantly decreases, indicating that Ag NPs have been successfully loaded in the m-TiO_2.

Furthermore, the effects of the $[Ag(NH_3)_2]NO_3$ concentration on the structure of Ag/m-TiO_2 heterostructures were also investigated, as shown in **Figure 7**. As shown in **Figure 7a**, increasing concentration of $[Ag(NH_3)_2]^+$ to 2×10^{-2} M, m-TiO_2 sphere was nearly completely capped by Ag particles and formed a core-shell structure. Further increasing the concentration to 2×10^{-1} M, it is obviously observed that large Ag particles with diameter of 50 nm attach on the m-TiO_2 surface (**Figure 7b**). The corresponding XRD patterns were shown as **Figure 7c**. Several well-resolved diffraction peaks appeared at 2θ= 38.0°, 44.2°, 64.3° and 77.2° are readily indexed to metal Ag with face-centered cubic structure (JCPDS card no. 04-0783). The intensity of Ag becomes stronger with the increasing of $[Ag(NH_3)_2]NO_3$ concentration, suggesting that the content of Ag was increased.

3.2 Photocatalytic performance

Ag/m-TiO_2 hybrids as photocatalysts were investigated to degrade methylene blue (MB). The C/C_0 versus irradiation time is plotted in **Figure 8a**. In the case of the Ag-1/m-TiO_2 catalyst, the MB completely destroyed only takes 25 min. However, with the increasing of Ag, the photocatalytic performance reduces. The reasonable explanation is that Ag particles wrapped on the surface of m-TiO_2 reducing the utilization of mesopores, consequently decreasing the contact area between the MB and the catalyst. In other words, only Ag particles play a catalytic role (Ag-2/m-TiO_2). Especially, the catalytic activity significantly reduced, even lower than m-TiO_2. This may be due to the large particle size of the Ag wrapped on m-TiO_2 surface, which reduces the adsorption rate of the light, consequently weakening the photocatalytic performance. **Figure 8b** shows UV-vis spectra for the degradation of the MB catalyzed by Ag-1/m-TiO_2 under UV light. The typical peak of MB at 665 nm disappears fast, suggesting that this sample exhibits excellent photocatalytic activity.

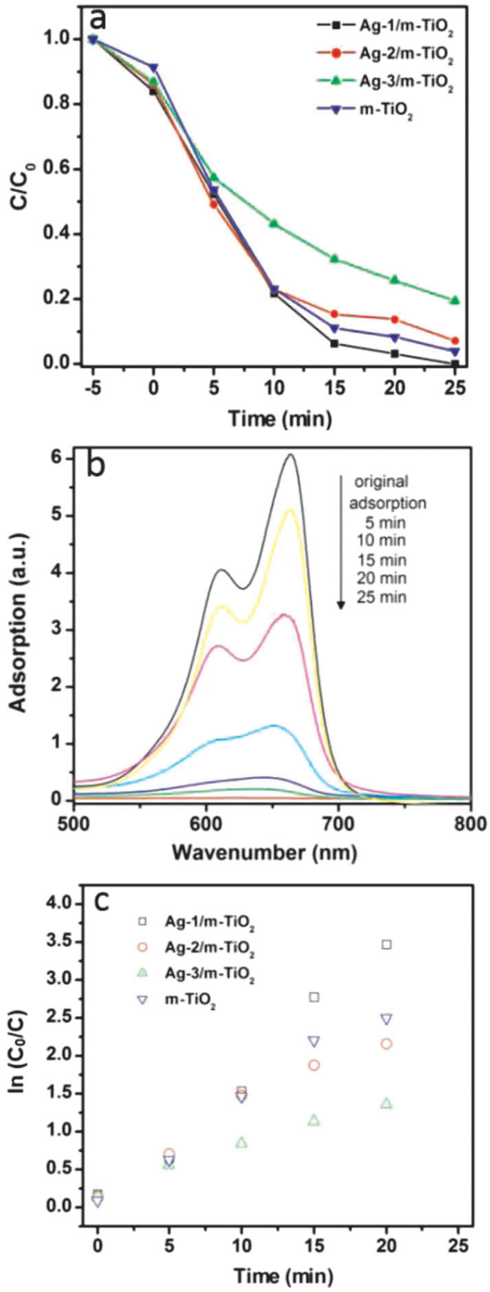

Figure. 8: a) Photocatalytic degradation of MB under UV light of different catalysts, b) time-dependent adsorption spectra of MB with Ag-1/m-TiO_2, c) the corresponding kinetic data for the degradation of MB

The photocatalytic degradation of MB allows for pseudo first-order kinetics, and the apparent degradation rate constant k could be determined by ln $(C_0/C) = kt$. The relationships between ln (C_0/C) and the reaction time of all the photocatalysts are linear, as shown in **Figure 8c**. It can be observed that Ag-1/m-TiO_2 posseses the highest apparent reaction rate constant, certifying the high photocatalytic activity, which is attributed

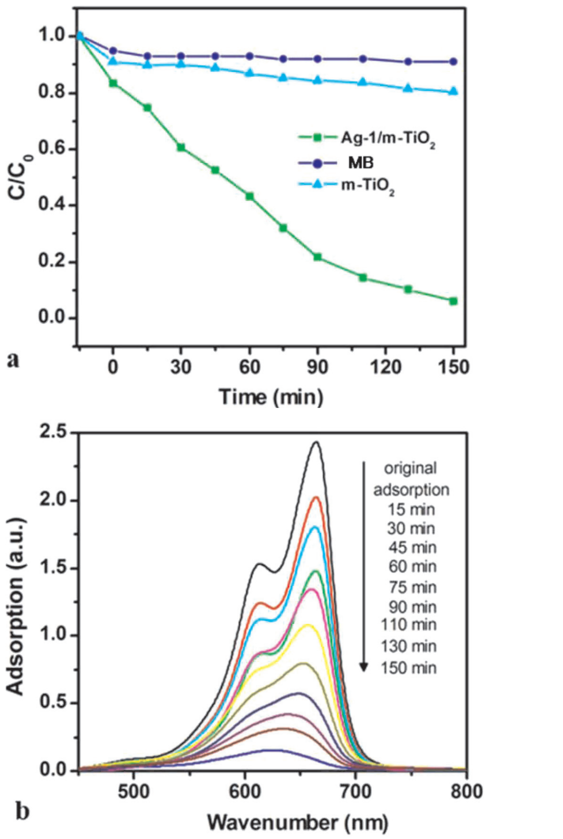

Figure 9: a) Photocatalytic degradation of MB under visible light of different catalysts, b) time-dependent adsorption spectra with Ag-1/m-TiO_2

to its unique structure. First, the large mesopores structure and specific surface area can enlarge the contact between the organics and photocatalyst. Secondly, the heterostructure is beneficial for the separation between photo-generated electron and hole.

Combined with the results of SEM (**Figure 2**) and phtocatalytic activity under UV light (**Figure 8**), Ag-1/m-TiO_2 was chosen as photocatalyst used under visible light irradiation. **Figure 9a** exhibits the degradation of MB with times. Compared with m-TiO_2, loading metallic Ag on the surface of m-TiO_2 spheres increases the photocatalytic performance. After 150 min of irradiation, 96 % MB was destroyed. It indicates that the Ag-TiO_2 heterojunction could enhance the electron-charge separation efficiency. **Figure 9b** shows the changes of the absorption spectra of the MB aqueous solution exposed to visible light for various times in the presence of Ag-1/m-TiO_2. Under visible-light illumination, the MB absorption rate rapid decreases at 665 nm.

4 DISCUSSION

UV-vis diffuse reflectance (DRUV-VIS) was used to further investigate the adsorption of products under visible light and UV light. The DRUV-VIS for Ag/m-TiO_2 and pure m-TiO_2 were compared, as displayed in **Figure 10a**. The pure m-TiO_2 spheres show the adsorption edges at about 390 nm, which is ascribed to the charge transfer from the valence band (mainly formed by 2p orbitals of the oxide anions) to the conduction band (mainly formed by $3d_{t2g}$ orbitals of the Ti^{4+} cations) and no adsorption can be observed in the visible-light region.[27] While for Ag/m-TiO_2, the high absorbance begins from 400 nm to the whole visible region, which is the typical features of the surface plasmon absorption of spatially restricted electrons from Ag NPs and further confirming the presence of the heterostructure between Ag and TiO_2. The absorbance in the range of visible region for the Ag-1/m-TiO_2 system increases and basically stays constant owing to the uniformly distributed Ag NPs on m-TiO_2. While for Ag-2/m-TiO_2, the absorption is even higher than that of Ag-1/m-TiO_2 at the beginning and then decreases gradually from 550 nm to 800 nm, suggesting that Ag NPs on m-TiO_2 are not evenly distributed.[28] In particular, the absorption of Ag-3/m-TiO_2 decreases significantly ascribed to large amount of Ag particles wrapped on m-TiO_2 resulting in the high energy surface is covered.

Under UV illumination, TiO_2 is activated and generates electron–hole pairs. Ag NPs have a favorable Fermi level (0.4V vs. normal hydrogen electrode NHE), which can serve as a good electron acceptor.[17] Thus, Ag can trap the photogenerated electron in the conduction band of m-TiO_2 for facilitating quick electron transfer and it is energetically favorable.[29] Consequently, it lowers the recombination of photo-induced charges, as exhibited in **Figure 10b**. Furthermore, The Fermi level shifts to more negative and renders Ag more reductive due to the accumulation of trapped electrons in Ag nanopaticles. Both the photogenerated electrons in TiO_2 as well as the trapped electrons in Ag will react with O_2, and yield some highly oxidative species, for example, peroxide

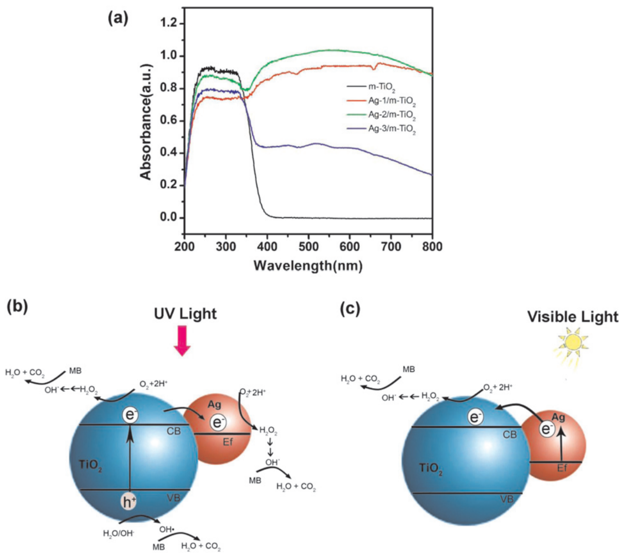

Figure 10: a) UV-vis diffuses reflectance spectra of Ag/m-TiO_2 composites and schematics of photocatalytic mechanism, b) UV light and c) visible light

(H_2O_2), which can further generate hydroxyl radical (OH·) and effectively degrade organic substrates. Simultaneously, the holes in the valence band of m-TiO_2 can react with H_2O or OH^- and also generate OH·, which then decompose MB. The degradation rate is much faster under UV illumination because both electrons and holes generated from m-TiO_2 can give contributions to the degradation of MB. Ag loaded in m-TiO_2 enlarges the interface area and improves the charge separation and consequently elevates the photocatalytic performance. For Ag/m-TiO_2 composite samples, Ag can trap the photogenerated electrons in the conduction band of m-TiO_2 and consequently prolongs the lifetime of holes in the valence band. However, the loading of Ag would also give adverse effects on the photocatalytic performance that Ag can be excited, generating electrons and then transfer back to m-TiO_2, which prevents the separation of charges in m-TiO_2. Therefore, the amount of Ag is a key to affect the photocatalytic performance.

Under UV–visible illumination (**Figure 10c**), MB molecules and nano-size Ag can both be excited by visible light, which results in self-photosensitization and hot electrons transferred to the conduction band of m-TiO_2, respectively. To further investigate the effects of visible light added, an enhancement factor EF, which is defined as $EF = k'_{\text{UV-vis}}/k'_{\text{UV}}$ is used as a reference. According to reference no. 8, the EF values of m-TiO_2 ad Ag-1/m-TiO_2 are 1.81 and 1.79, respectively, which is inversely related to the specific decay rate under visible illumination. It implies the smaller EF, better photocatalytic performance under UV–visible irradiation.

According to the above discussions, it is concluded that the loading Ag composites is indeed improving the photocatalytic performance of m-TiO_2.

5 CONCLUSIONS

In summary, Ag/m-TiO_2 heterostructure photocatalysts have been prepared by a facile method. Ag NPs homogeneously distribute on the m-TiO_2 spheres. The $[Ag(NH_3)_2]NO_3$ concentration is critical for controlling the particle size and the distribution of Ag. Moreover, the hybrids with large pores and a high specific surface area determine Ag/m-TiO_2 as a candidate for the catalyst. The photocatalytic measurement results demonstrate that the Ag-1/m-TiO_2 manifests its outstanding performance under both UV and visible light, compared with m-TiO_2.

Acknowledgements

This work was supported by the National Natural Science Foundation of China (No. 21076094 and 21673097).

6 REFERENCES

[1] A. F. K. Honda, Electrochemical photolysis of water at a semiconductorelectrode, Nature, 238 (**1972**), 37–38

[2] J. M. Zhang, X. Jin, P. I. Morales-Guzman, X. Yu, H. Liu, H. Zhang, L. C. Razzari, P. Jerome, Engineering the absorption and field enhancement properties of Au-TiO_2 nanohybrids via whispering gallery mode resonances for photocatalytic water splitting, ACS Nano, 10 (2016), 4496–4503, doi:10.1021/acsnano.6b00263

[3] A. Gomathi, S. R. C. Vivekchand, A. Govindaraj, C. N. R. Rao, Chemically bonded ceramic oxide coatings on carbon nanotubes and inorganic nanowires, Adv. Mater., 17 (**2005**), 2757–2761

[4] A. Shahat, E. A. Ali, M. E. Shahat, Colorimetric determination of some toxic metal ions in post-mortem biological samples, Sensors and Actuators B: Chemical, 221 (**2015**), 1027–1034, doi:10.1016/j.snb.2015.07.032

[5] C. Wang, C. Shao, L. Wang, L. Zhang, X. Li, Y. Liu, Electrospinning preparation, characterization and photocatalytic properties of Bi_2O_3 nanofibers, J. Colloid Interf. Sci., 333 (**2009**), 242–248

[6] X. Li, P. Liu, Y. Mao, M. Xing, J. Zhang, Preparation of homogeneous nitrogen-doped mesoporous TiO_2 spheres with enhanced visible-light photocatalysis, Appl. Cataly. B, Environ., 164 (**2015**), 352–359, doi:10.1016/j.apcatb.2014.09.053

[7] V. Iliev, D. Tomova, A. Eliyas, S. Rakovsky, M. Anachkov, L. Petrov, Enhancement of the activity of TiO_2-based photocatalysts: a review, Bulgarian Chem. Commun., 47 (**2015**), 1–5

[8] Y. Z. He, P. Basnet, S. E. H. Murph, Y. P. Zhao, Ag Nanoparticle Embedded TiO_2 Composite Nanorod Arrays Fabricated by Oblique Angle Deposition, Toward Plasmonic Photocatalysis, ACS Appl. Mater. Interf., 5 (**2013**), 11818–11827

[9] Y. C. Liang, C. C. Wang, C. C. Kei, Y. C. Hsueh, W. H. Cho, T. P. Perng, Photocatalysis of Ag-Loaded TiO_2 nanotube arrays formed by atomic layer deposition, J. Phys. Chem. C, 115 (**2011**), 9498–9502

[10] D. Chen, L. Cao, F. Huang, P. Imperia, Y. B. Cheng, R. A. Caruso, Synthesis of monodisperse mesoporous titania beads with controllable diameter, high surface areas, and variable pore diameters (14–23 nm), J. Am. Chem. Soc., 132 (**2010**), 4438–4444

[11] O. K. Dalrymple, E. Stefanakos, M. A. Trotz, D. Y. Goswami, A review of the mechanisms and modeling of photocatalytic disinfection, Appl. Cataly. B, Environ., 98 (**2010**), 27–38

[12] H. F. Shi, Y. C. Yua, Y. Zhanga, X. J. Feng, X. Y. Zhao, H. Q. Tan, S. U. Khana, Y.G. Lia, E. B. Wang, Polyoxometalate/TiO_2/Ag composite nanofibers with enhanced photocatalytic performance under visible light, Applied Catalysis B, Environmental, 221 (**2018**), 280–289, doi:10.1016/j.apcatb.2017.09.027

[13] Y. R. Fang, Y. Jiao, K. L. Xiong, R. B. Ogier, Z. J. Yang, S. W. Gao, A. B. Dahlin, M. Käll, Plasmon enhanced internal photoemission in antenna-spacer-mirror based Au/TiO_2 nanostructures, Nano Lett., 15 (**2015**), 4059–4065, doi:10.1021/acs.nanolett.5b01070

[14] S. Dutta, R. Sahoo, C. Ray, S. Sarkar, J. Jana, Y. Negishi, T. Pal, Biomolecule-mediated CdS-TiO_2-reduced graphene oxide ternary nanocomposites for efficient visible light-driven photocatalysis, Dalton T., 44 (**2014**), 193–201

[15] B. A. Lu, X. D. Li, T. H. Wang, E. Q. Xie, Z. Xu, WO_3 nanoparticles decorated on both sidewalls of highly porous TiO_2 nanotubes to improve UV and visible-light photocatalysis, J. Mater. Chem. A, 1 (**2013**), 3900–3906

[16] Y. Bi, H. Hu, S. Ouyang, Z. Jiao, G. Lu, J. Ye, Selective growth of Ag_3PO_4 submicro-cubes on Ag nanowires to fabricate necklace-like heterostructures for photocatalytic applications, J. Mater. Chem., 22 (**2012**), 14847–14850

[17] P. V. Kamat, Meeting the Clean Energy Demand, Nanostructure Architectures for Solar Energy Conversion, J. Phys. Chem. C, 111 (**2007**), 2834–2860

[18] S. Ko, J. Nanosci. Photochemical Synthesis, Characterization and Enhanced Visible Light Induced Photocatalysis of Ag Modified TiO_2 Nanocatalyst, Nanotechno., 14 (**2014**), 6923–6928

[19] P. Shahini, A. A. Ashkarran, Immobilization of plasmonic Ag-Au NPs on the TiO_2 nanofibers as an efficient visible-light photocatalyst, Colloids and Surfaces A, 537 (**2018**), 155–162, doi:10.1016/j.colsurfa.2017.10.009

[20] Y. J. Li, L. M. Yu, N. Li, W. F. Yan, X. T. Li, Heterostructures of Ag_3PO_4/TiO_2 mesoporous spheres with highly efficient visible light

photocatalytic activity, J. Colloid Interf. Sci., 450 (**2015**), 246–253, doi:10.1016/j.jcis.2015.03.016

[21] J. Ma, X. Guo, Y. Zhang, H. Ge, Catalytic performance of TiO_2@Ag composites prepared by modified photodeposition method, Chem. Eng. J., 258 (**2014**), 247–253

[22] J. C. Vartuli, K. D. Schmitt, C.T. Kresge, W. J. Roth, M. E. Leonowicz, S. B. McCullen, S. D. Hellring, J. S. Beck, J. L. Schlenker, Effect of Surfactant/Silica Molar Ratios on the Formation of Mesoporous Molecular Sieves: Inorganic Mimicry of Surfactant Liquid-Crystal Phases and Mechanistic Implications, Chem. Mater., 6 (**1994**), 2317–2326

[23] Y. Chi, J. C. Tu, M. G. Wang, X. T. Li, Z. K. Zhao, One-pot synthesis of ordered mesoporous silver nanoparticle/carbon composites for catalytic reduction of 4-nitrophenol, J. Colloid Interf. Sci., 423 (**2014**), 54–59

[24] Y. Xia, F. Li, Y. Jiang, M. Xia, B. Xue, Y. Li, Interface actions between TiO_2 and porous diatomite on the structure and photocatalytic activity of TiO_2-diatomite, Appl. Surf. Sci., 303 (**2014**), 290–296

[25] F. Zhang, Y. Pi, J. Cui, Y. Yang, X. Zhang, N. Guan, Unexpected Selective Photocatalytic Reduction of Nitrite to Nitrogen on Silver-Doped Titanium Dioxide, J. Phys. Chem. C, 111 (**2007**), 3756–3761

[26] S. M. Mukhopadhyay, S. H. Garofalini, Surface studies of TiO_2-SiO_2 glasses by X-Ray photoele ctron-spectroscopy, J. Non-Cryst. Solids, 126 (**1990**), 202–208

[27] H. Gerischer, A. Heller, The role of oxygen in photooxidation of organic-molecules on semiconductor particles, J. Phys. Chem., 95 (**1991**), 5261–5267

[28] N. Sobana, M. Muruganadham, M. Swaminathan, Nano-Ag particles doped TiO_2 for efficient photodegradation of Direct azo dyes, J. Mol. Cataly. A, Chem., 258 (**2006**), 124–132

[29] A. Takai, P. V. Kamat, Capture, Store, and Discharge. Shuttling Photogenerated Electrons across TiO_2-Silver Interface, ACS Nano, 5 (**2011**), 7369–7376